



**HAL**  
open science

# **On-line inductively coupled plasma-atomic emission spectroelectrochemistry: Real-time element-resolved electrochemistry**

Borhan Bin Mohamad Sultan, Oumaïma Gharbi, Kevin Ogle, Junsoo Han

## **► To cite this version:**

Borhan Bin Mohamad Sultan, Oumaïma Gharbi, Kevin Ogle, Junsoo Han. On-line inductively coupled plasma-atomic emission spectroelectrochemistry: Real-time element-resolved electrochemistry. *Current Opinion in Electrochemistry*, 2023, 41, pp.101350. <10.1016/j.coelec.2023.101350>. <hal-04211090>

**HAL Id: hal-04211090**

**<https://hal.sorbonne-universite.fr/hal-04211090v1>**

Submitted on 1 Oct 2025

**HAL** is a multi-disciplinary open access archive for the deposit and dissemination of scientific research documents, whether they are published or not. The documents may come from teaching and research institutions in France or abroad, or from public or private research centers.

L'archive ouverte pluridisciplinaire **HAL**, est destinée au dépôt et à la diffusion de documents scientifiques de niveau recherche, publiés ou non, émanant des établissements d'enseignement et de recherche français ou étrangers, des laboratoires publics ou privés.



Distributed under a Creative Commons CC BY-NC 4.0 - Attribution - Non-commercial use - International License

1 **On-line inductively coupled plasma-atomic emission spectroelectrochemistry: Real-time**  
2 **element-resolved electrochemistry**

3 <sup>a,b</sup>Borhan BIN MOHAMAD SULTAN, <sup>c</sup>Oumaïma GHARBI, <sup>a</sup>Kevin OGLE, <sup>d</sup>Junsoo HAN

4 <sup>a</sup>Chimie ParisTech, PSL University, *Institut de Recherche Chimie Paris*, CNRS, F-75005 Paris,  
5 France

6 <sup>b</sup>*Institut de la Corrosion* (French Institute of Corrosion), F-29200 Brest, France

7 <sup>c</sup>*Sorbonne Université*, CNRS, *Laboratoire de Réactivité de Surface*, LRS, F-75005 Paris, France

8 <sup>d</sup>*Sorbonne Université*, CNRS, *Laboratoire Interfaces et Systèmes Electrochimiques*, LISE, F-75005  
9 Paris, France

10

11 **Abstract**

12 Electrochemical techniques are coupled with inductively coupled plasma atomic emission  
13 spectrometry (ICP-AES) for in-line electrolyte analyses. In this way, a direct measurement of the  
14 elemental dissolution rates in real-time or element-resolved electrochemistry can be carried out,  
15 complementary to conventional electrochemical measurements of current and potential. This  
16 methodology can be used to obtain the element-specific reaction mechanisms under either  
17 spontaneous or polarized conditions up to part-per-billion level resolution with applications in diverse  
18 domains of corrosion science and interfacial reactivity. This review aims to summarize recent research  
19 activities using ICP coupled with other analytical techniques to answer specific questions on the  
20 mechanism of degradation of materials in aqueous or organic environments including the dissolution  
21 of metal oxides, catalysis, reaction stoichiometry, electrochemical kinetics, and photoelectrochemical  
22 reactivity.

23 **Keywords:** AESEC; ICP-AES; kinetics; catalysis,

24

## 25 **Introduction**

26 Electrochemical methods and concepts are commonly used to measure and interpret  
27 interfacial electron exchange processes. The total current ( $i_e$ ) is a remarkable measurement of the rate  
28 of electron exchange and can be obtained with an exceptional degree of accuracy and time resolution.  
29 However, in addition to the rate of electron exchange, often we would like to know how the current is  
30 distributed among the various elements of a material, distinguish oxide formation from dissolution,  
31 separate the anodic and cathodic partial process, observe non-faradaic reactions such as oxide  
32 dissolution, particle detachment, or measure dissolution rates at open circuit when the faradaic current  
33 is by definition equal to zero.

34 To obtain element-resolved electrochemical responses (*i.e.*, decoupling elemental anodic  
35 dissolution from the total electrochemical current,  $i_e$ ), spectroelectrochemical methods have been  
36 developed coupling an electrochemical flow cell with ICP-AES (AESEC, atomic emission  
37 spectroelectrochemistry) or mass spectrometer, ICP-MS, (ASEC, atomic spectroelectrochemistry)<sup>1,2</sup>  
38 and have been extensively reviewed.<sup>3,4</sup> In this review, recent advancements in coupling the basic  
39 spectroelectrochemical techniques with other analytical techniques are highlighted, while also  
40 discussing some of the novel applications of ICP-MS for electrocatalysis. A schematic image  
41 illustrating the principle of on-line ICP-AES measurement (*i.e.*, AESEC) coupled with other  
42 analytical techniques is presented in **Fig. 1**.<sup>1,3,5</sup>

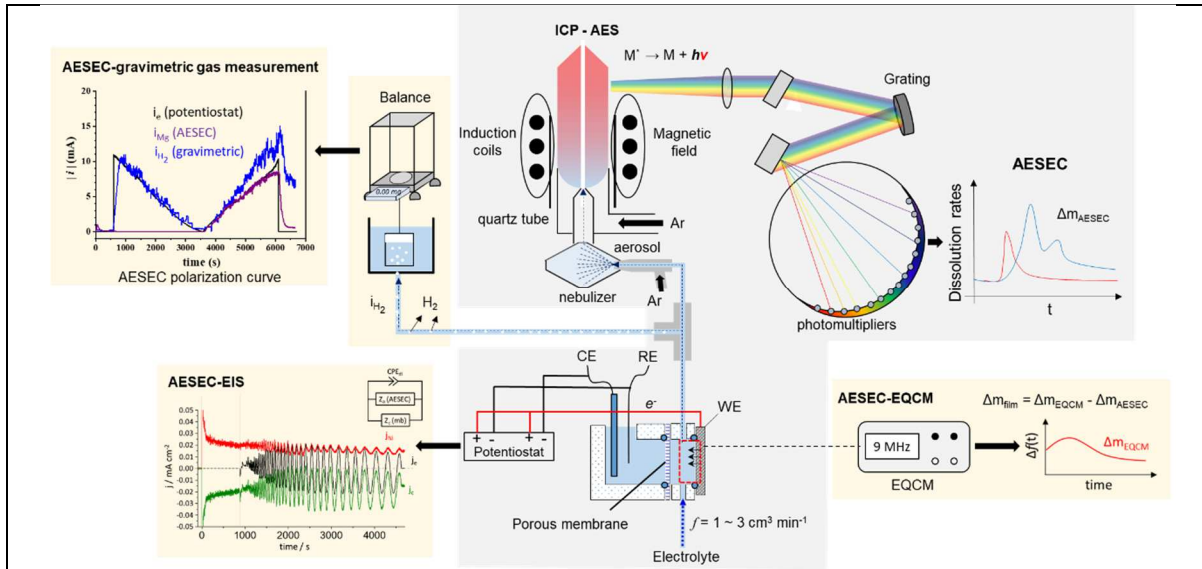


**Fig. 1.** Schematic image of the principles of the AESEC coupled with other analytical and electrochemical techniques. The electrolyte containing dissolved species from the (electro)chemical reaction is transported to an Ar source plasma, then the dissolved species M is atomized and exited to an energy state of  $M^*$ . The excited atom  $M^*$  emits electromagnetic radiation with an element-specific wavelength when it decays to the ground energy state. In the case of the ASEC (ICP-MS),<sup>2</sup> the free ions produced in the plasma are separated by the mass-to-charge ratio with a quadrupole mass spectrometer (not shown here). The intensity of the emitted radiation or ions may be calibrated to determine the concentration of the original solution.

43

44 **AESEC coupled with other analytic techniques for aqueous corrosion**

45 The AESEC technique provides real-time elemental dissolution rate profiles for multiple  
 46 elements simultaneously with corresponding electrochemical measurement and/or control of potential  
 47 and current.<sup>1,3,4,6</sup> For example, an open circuit AESEC dissolution profile gives the contribution of  
 48 each element to the overall spontaneous corrosion rate simultaneously with the open circuit potential  
 49 trend, frequently allowing a more precise interpretation of the latter. This *operando* technique has  
 50 been used in the field of aqueous corrosion of different alloys such as stainless steels,<sup>1,7</sup> bipolar  
 51 plates,<sup>8</sup> Ni-,<sup>9,10</sup> Al-,<sup>11,12</sup> Mg-,<sup>13,14</sup> Zn-,<sup>15,16</sup> Cu-based alloys,<sup>17,18</sup> multi-principal element alloys,  
 52 <sup>19,20,21,22,23,24</sup> additively manufactured alloys,<sup>25</sup> noble metals,<sup>26,27,28</sup> surface pretreatment,<sup>29,30,31,32</sup> and  
 53 electrochemical texturing of thin films for photovoltaic applications (ASEC)<sup>33</sup> which have been  
 54 reviewed elsewhere.<sup>2,3,4</sup>

55           Limitations persist such as a lack of direct information<sup>a1</sup> on the deposition kinetics of surface  
56 films (*e.g.*, oxides, coatings), quantification of gas formation, difficulty in determining oxidation  
57 states, etc. Recent developments have adopted the coupling of AESEC to a few other analytical  
58 techniques to overcome these challenges. This section introduces the readers to such advances  
59 involving the coupling of the AESEC technique for different applications beyond aqueous corrosion  
60 research.

61

### 62 *AESEC-gravimetric H<sub>2</sub> measurement*

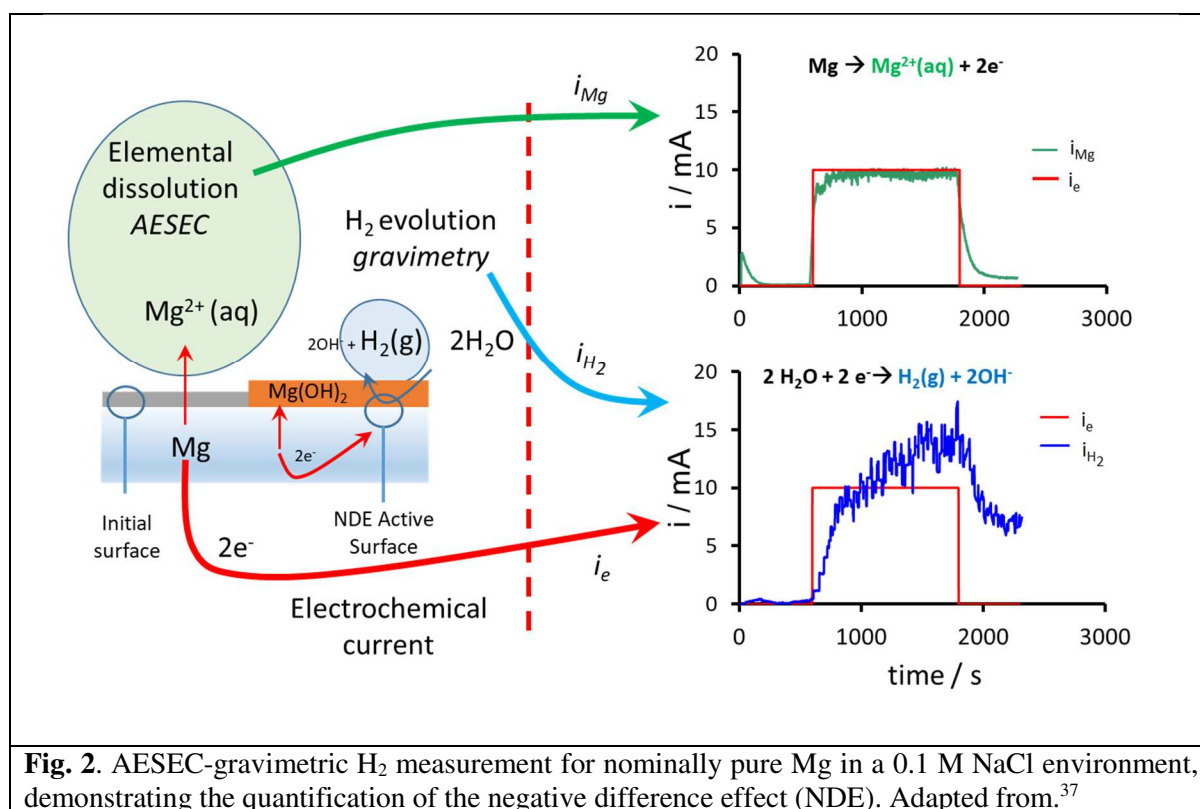
63           The hydrogen evolution reaction (HER) can occur when a metallic material is exposed to  
64 atmospheric or aqueous environments leading to surface defects. This is critical in the case of alloy  
65 coatings because local damage to the coating causes a galvanic coupling between the alloy coating  
66 and the metal substrate, resulting in an enhanced HER over a large applied cathodic potential. In the  
67 case of Mg-based alloys, the evolution of hydrogen during the dissolution limits the use of Mg-based  
68 alloys as anodic material in batteries or sacrificial anodes, as well as the application of biocompatible  
69 alloys. The HER acts as a parasitic reaction in these applications, reducing battery efficiency and  
70 causing defects when used as bio-implants.

71           Novel experimental protocols for the real-time quantification of the HER have been  
72 developed with AESEC coupled with time-resolved volumetry<sup>34</sup> and more recently, with gravimetric  
73 H<sub>2</sub> measurement using analytical grade balance.<sup>35</sup> The gravimetric H<sub>2</sub> measurement coupled with the  
74 AESEC technique (**Fig. 1**) can give complete stoichiometric information during the reaction by  
75 providing the anodic component ( $i_a$ , AESEC), the cathodic component ( $i_c$ , gravimetric H<sub>2</sub>  
76 measurement), and the total charge ( $i_e$ , potentiostat). This coupling was applied to a galvanized steel  
77 in HCl where the elemental dissolution and HER rate profile were obtained with several kinetic  
78 regimes including the dissolution of the alloy coating, the dissolution of the nanometric Fe<sub>2</sub>Al<sub>5</sub>  
79 intermetallic layer, and the dissolution of the steel substrate.<sup>36</sup> This methodology was also used to

---

<sup>a</sup> It could be obtained indirectly by mass-charge balance in some cases.

80 understand the stoichiometry of anodic hydrogen evolution of Mg alloys (*i.e.*, negative difference  
 81 effect, NDE) as described in **Fig. 2**.<sup>37</sup> Using this novel coupling, it was demonstrated that  
 82 electrochemical dissolution occurs through an intact Mg-based corrosion product film while HER  
 83 occurs independently in regions where the film breaks down induced by anodic polarization.  
 84



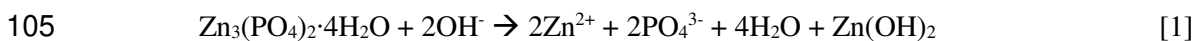
85

### 86 AESEC-electrochemical quartz microbalance

87 The electrochemical quartz microbalance (EQCM) monitors mass changes at the reaction  
 88 interface with less than one monolayer level (ng cm<sup>-2</sup>), making it useful for the quantification of  
 89 (electro)deposition processes.<sup>38</sup> Coupling AESEC with EQCM measures simultaneously the real-time  
 90 mass changes caused by insoluble film formation (deposition) and the element-resolved  
 91 dissolution.<sup>39,40</sup> In this way, the total mass change (mass gain + mass loss) can be monitored by  
 92 EQCM ( $\Delta m_{EQCM}$ ), and mass change caused by dissolution (mass loss) can be directly measured by  
 93 AESEC ( $\Delta m_{AESEC}$ ), yielding the film formation rate as  $\Delta m_{film} = \Delta m_{EQCM} - \Delta m_{AESEC}$  (**Fig. 1**). This  
 94 coupling can be used to investigate the elemental contribution of the conversion coating formation

95 process<sup>41,42</sup> which involves simultaneously the substrate (and/or the film) dissolution and the film  
96 formation reactions.

97 An example of the use of combined AESEC-EQCM is given in **Fig. 3** to determine the  
98 stoichiometry and dissolution rate of Zn-phosphate conversion coatings in an alkaline solution.<sup>39,43</sup>  
99 Alkaline resistance is an important property of the conversion coating which may encounter an  
100 alkaline environment either during the cathodic deposition of a primer layer or during underpaint  
101 corrosion by a mechanism of cathodic delamination. For the mono-cation case (**Fig. 3(a)**), AESEC  
102 technique permits a clear characterization of the stoichiometry: first there is an equimolar dissolution  
103 rates of the  $Zn^{2+}$  and  $PO_4^-$  observed for  $t < 180$  s confirming the stoichiometry of the reaction as  
104 follows:



106 For  $t > 180$  s, the Zn dissolution rate exceeds that of P due to the dissolution of  $Zn(OH)_2$  forming  
107  $Zn(OH)_4^{2-}$  by  $Zn(OH)_2 + 2 OH^- \rightarrow Zn(OH)_4^{2-}$ . The mass change caused by the  $Zn(OH)_2$  formation,  
108  $\Delta m_{Zn(OH)_2}$ , is calculated by the difference between  $\Delta m_{EQCM}$  and  $\Delta m_{AESEC}$ , given in the right part of **Fig.**  
109 **3**. The  $\Delta m_{Zn(OH)_2}$  transient in **Fig. 3(a)** indicates the  $Zn(OH)_2$  formation coupled with its dissolution;  
110 thus the mass of the  $Zn(OH)_2$  passes through a maximum around  $t = 180$  s.

111 **Figs. 3(b)** and **3(c)** are the bi-cations cases showing the effect of  $Ni^{2+}$  and  $Mn^{2+}$ , respectively,  
112 often added to the conversion coating bath to improve the physical and chemical properties of the  
113 coating.<sup>42</sup> In both cases, the dissolution rate of the phosphate conversion coating is markedly reduced  
114 due to the formation of more stable  $Mn(OH)_2$  that was also detected by *in situ* Raman spectroscopy.<sup>44</sup>

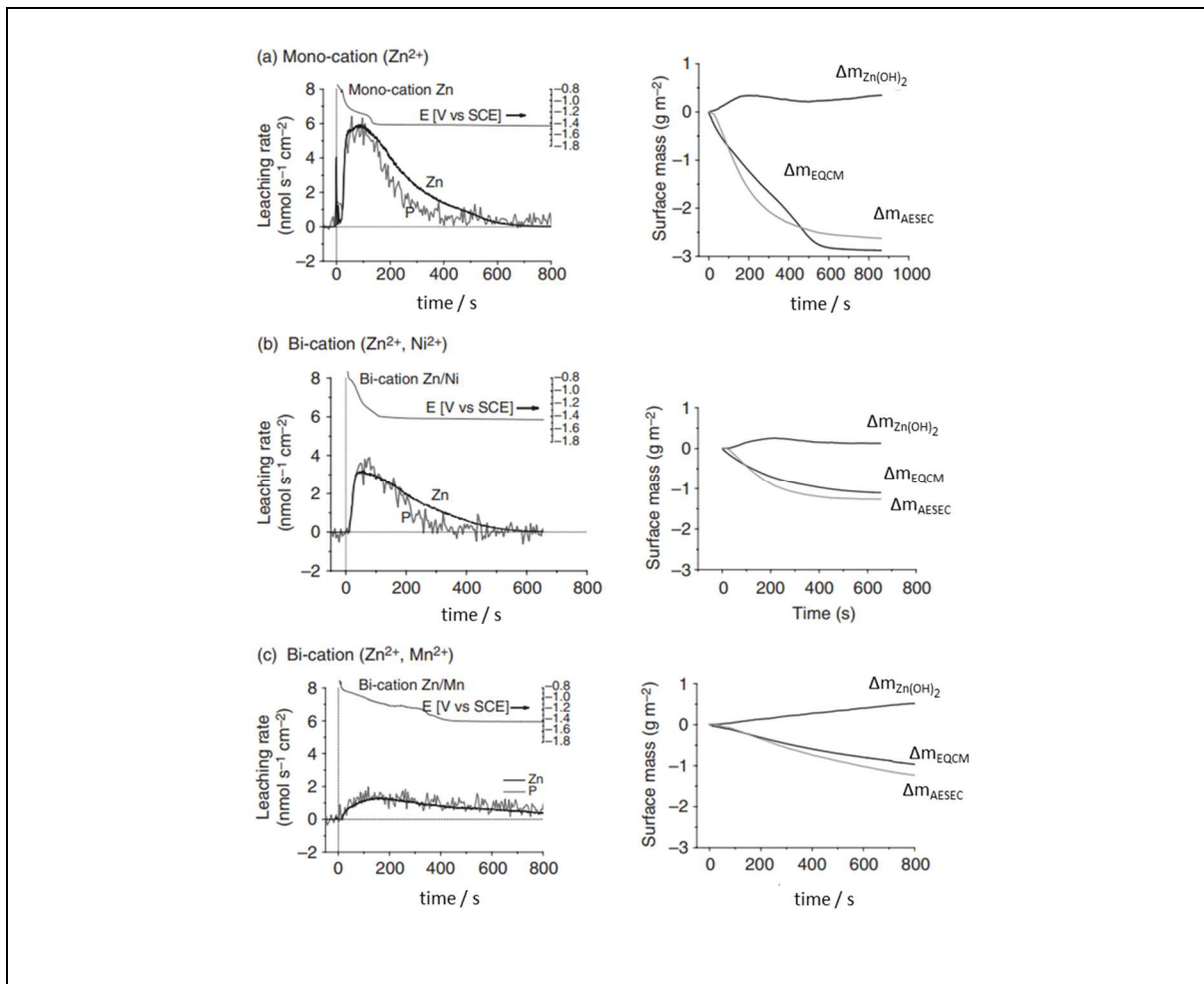


**Fig. 3.** Left column: elemental dissolution (leaching) rates profiles, right column: mass changes monitored by EQCM ( $\Delta m_{EQCM}$ ) and AESEC ( $\Delta m_{AESEC}$ ) for various phosphate layer compositions for the Zn-phosphate conversion coating formation reaction in deaerated 0.1 M NaOH solution. (a): Mono-cation ( $Zn^{2+}$ ); (b) bi-cations ( $Zn^{2+}$ ,  $Ni^{2+}$ ); and (c) bi-cations ( $Zn^{2+}$ ,  $Mn^{2+}$ ). The  $\Delta m_{Zn(OH)_2}$  curves represent the mass of the hydroxide intermediate ( $\Delta m_{EQCM} - \Delta m_{AESEC}$ ). Adapted from.<sup>39</sup>

115

116 *AESEC-electrochemical impedance spectroscopy*

117 Electrochemical impedance spectroscopy (EIS) can give kinetic information about a steady-

118 state reaction system. Interfacial properties obtained from the EIS spectra are often used to quantify

119 the kinetic processes including corrosion rates, resistance, and thickness of the surface film.<sup>45</sup>

120 Coupling EIS with AESEC provides element-resolved kinetic information.<sup>46,47</sup> It also allows to

121 distinguish the anodic and cathodic dissolution mechanisms on the one hand, and between dissolution

122 and film formation on the other.<sup>48,49</sup> Recently, element-resolved EIS plots of pure Ni and Fe have been

123 investigated using the AESEC-EIS methodology to quantitatively distinguish anodic (metal

124 dissolution) and cathodic (HER) reactions in sulfuric acid media.<sup>50</sup> In this case, the intermediate short-  
125 lived adsorbed species (*e.g.*, FeH<sub>ads</sub>, NiH<sub>ads</sub>)<sup>51</sup> could be ascertained by calculating the impedance of  
126 each reaction as:

$$127 \quad Z_{j_M} = \left| \frac{\Delta E}{\Delta j_M} \right| (\cos \varphi + j \sin \varphi) \quad [2]$$

128 where  $Z_{j_M}$  is the impedance of equivalent elemental current density  $j_M$  (M can be an element or H<sub>2</sub>)  
129 and  $\varphi$  is the phase angle of the EIS measurement. In **Eq. 2**,  $\Delta j_M$  was determined from the analog  
130 sinusoidal signal of  $j_M$  obtained by the AESEC data acquisition system, and used as a transfer function  
131 between the electrochemical and spectroscopic measurements.<sup>52</sup> In the absence of insoluble species  
132 formation, this permits the calculation of the anodic component of impedance ( $Z_a$ ) from the  
133 electrochemical dissolution, and the cathodic component of impedance ( $Z_c$ ) from the reduction of the  
134 electrolyte, as described in **Fig. 1**. In this case, element-resolved EIS plots (*e.g.*, Nyquist or Bode)  
135 may be obtained to shed light on elemental dissolution kinetics. A low-frequency loop in the Nyquist  
136 diagram is often attributed to the oxidation of this intermediate species or hydrogen evolution.<sup>50</sup> The  
137 element-resolved Bode plot for pure Ni and pure Fe in sulfuric acid showed that the low-frequency  
138 impedance is dominated by the cathodic impedance  $Z_c$ .<sup>50</sup>

139

## 140 **A(E)SEC for other fields of electrochemistry**

### 141 *Photoelectrochemistry and catalysts*

142 Photocorrosion of metal oxides is a non-negligible process for photoelectrochemical water  
143 splitting for energy applications, influencing the durability and overall efficiency of devices.  
144 Conventional electrochemical measurements to investigate the degradation mechanism of the  
145 photoelectrochemical water splitting are limited because of either insufficient resolution due to stable  
146 metal oxide materials yielding non-significant changes in electrochemical response or lack of  
147 elemental-specific contribution to photocorrosion.<sup>53</sup> To this end, electrochemical measurements  
148 coupled with on-line ICP-MS (ASEC) using an electrochemical scanning flow cell have been used to

149 monitor the photoelectrochemical responses of semiconducting oxides.<sup>54,55,56</sup> For example, it was  
150 reported that Zn dissolution from polar ZnO was accelerated by the UV irradiation at pH = 8 whereas  
151 nonpolar ZnO showed significantly less photocorrosion, thus demonstrating the possibility of direct  
152 quantitative monitoring of the photon-induced dissolution of the facet-tuned surface film.<sup>53</sup> Another  
153 example involves significant dissolution of WO<sub>3</sub> which was monitored during photoelectrochemical  
154 water splitting where the dissolved W was found to be proportional to the applied charge.<sup>52</sup>

155 Elemental dissolution profiles of metal oxide catalysts were also investigated by ICP-AES  
156 coupled with an oxygen sensor to measure the catalytic activity of the oxygen evolution reaction  
157 (OER).<sup>57</sup> In this way, elemental dissolution rates of Ni and Co from NiCoO<sub>2</sub> in 1 M KOH; Co from  
158 Co<sub>3</sub>O<sub>4</sub> in 1 M KOH; and Ir from IrO<sub>2</sub> OER catalyst in 0.1 M HClO<sub>4</sub> could be simultaneously  
159 monitored with potential vs. time during galvanostatic hold at 10 mA cm<sup>-2</sup> for ~8000 s.

160 The anodically formed (at different time durations) topmost atomic layers of IrO<sub>3</sub> for the OER  
161 were characterized simultaneously by ICP-MS to investigate the stability and activity of the material  
162 during and toward the reaction.<sup>58</sup> The result was then further complemented by combined *ex situ*  
163 characterizations, demonstrating that longer anodic polarization increases the stability at the detriment  
164 of decreased catalytic activity.<sup>59</sup> All this demonstrates the capability of *in situ* ICP-  
165 photoelectrochemistry to investigate the stability of the catalyst and co-catalyst materials in various  
166 environments.

167

### 168 *Battery materials*

169 The analysis of the activity and stability of the transition metal-based oxide materials for  
170 energy application relies heavily on the conventional electrochemical test and *ex situ* electrolyte  
171 analysis for the quantification of the dissolved species. In this case, dynamic elemental reactivity  
172 during charge-discharge cycles cannot be directly monitored. The stationary probe rotating disk  
173 electrode (RDE) coupled to ICP-MS (SPRDE-ICP-MS) was introduced to simultaneously monitor the  
174 metal oxide dissolution and deintercalation kinetics of the working cations.<sup>60</sup> This technique also  
175 makes it possible to monitor the degradation of the organic solvent, usually not possible *via*  
176 conventional electrochemical measurements. Co dissolution from LiCoO<sub>2</sub> cathode material in 1.2 M

177 LiPF<sub>6</sub> in 3:7 ethylene carbonate/ethyl methyl carbonate organic solvent was quantitatively evaluated  
178 by SPRDE-ICP-MS using an RDE-specific stationary probe, organic environment-appropriate tubing  
179 and nebulization equipment. This method was also used to monitor the kinetics of dissolved Mg<sup>2+</sup>  
180 cations throughout the MgCr<sub>2</sub>O<sub>4</sub> deintercalation process for Mg-ion batteries in 0.2 M LiTFSI.<sup>60</sup>

181

### 182 *Surface pretreatment*

183 Non-faradaic particle release during corrosion or surface treatment processes cannot be  
184 generally detected by conventional electrochemical measurement and has been often overlooked.  
185 Over the years, non-faradaic particle release has gained considerable interest, particularly in the  
186 context of dealloying and surface treatment of Al alloys.<sup>61</sup> AESEC has demonstrated the ability to  
187 provide quantitative analysis on non-faradaic processes. Element- and time-resolved particle analysis  
188 by the AESEC technique is possible with fast data acquisition (1000 Hz level) detecting the element-  
189 specific transient events within this time frame.

190 Mokaddem *et al.* observed the surface detachment of Cu-rich particles while monitoring the  
191 potential-controlled local dissolution of an Al-Cu-Mg alloy in NaCl.<sup>62</sup> Serdechnova *et al.* qualitatively  
192 measured Al particles of various nominal sizes released from Al particle-enriched patinas.<sup>63</sup> Gharbi *et*  
193 *al.* also qualitatively measured the release of different types of intermetallic particles during alkaline  
194 etching of an AA2024.<sup>29,64</sup> Statistical analysis revealed a strong correlation between different  
195 elemental signals and intensities that were found to be consistent with expected intermetallic particles  
196 such as Al<sub>2</sub>CuMg and Al<sub>7</sub>Cu<sub>2</sub>Fe (**Fig. 4**). These findings are promising in the context of materials  
197 design because they demonstrate the possibility to analyze a large population of particle composition  
198 and get access to alloy composition (intermetallic size, composition, and proportions).

199

200

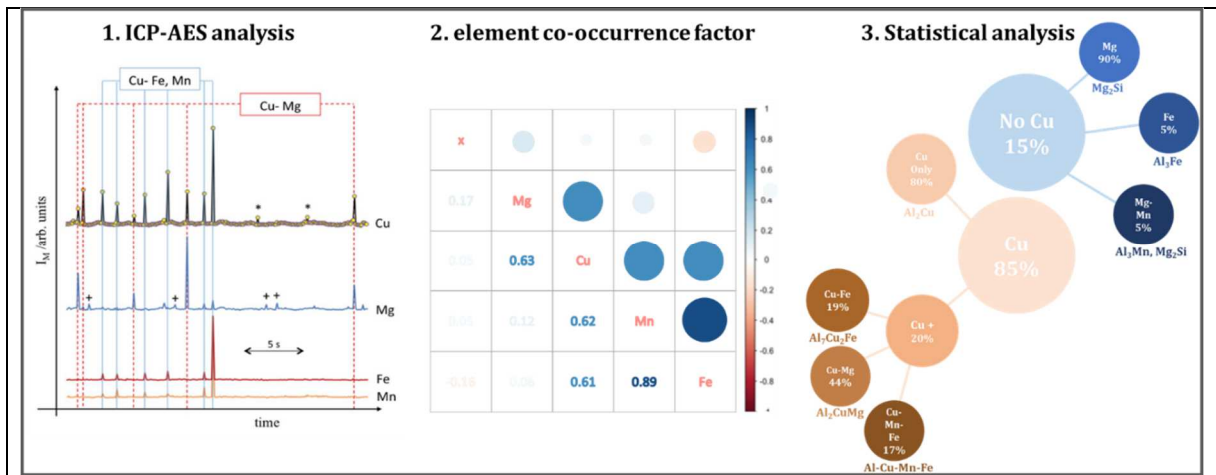


**Fig. 4.** Schematic illustration of the AESEC elemental dissolution rate transients for Cu, Mg, Fe, and Mn of an AA2024 alloy exposed to 1.2 M NaOH at  $T = 60^{\circ}\text{C}$ . The data was acquired at 10 Hz to provide greater temporal resolution on transient events and each peak corresponds to a transient particle release event. The statistical analysis of such peaks revealed a strong co-occurrence between certain elements and their intensities. For example, there were frequent appearance of simultaneous Mg and Cu peaks, probably due to  $\text{Al}_2\text{CuMg}$  particle release. The high-intensity peaks were linked to large intermetallic particles with stoichiometry correlated to what is reported in the literature. The figure is taken from.<sup>63</sup>

201

202 **Perspectives and closing remarks**

203 AESEC and electrochemical methods can be adapted with a few other complementary on-line  
 204 techniques to answer contemporary scientific questions, such as the degradation mechanism of  
 205 materials used in energy applications. Although the current experimental setup of AESEC is  
 206 somewhat limited to macroscopic scale electrochemical analysis<sup>65</sup>, this technique could however be  
 207 extended to the monitoring of localized reactions, for example by coupling it with atomic force  
 208 microscopy.<sup>66</sup> The determination of the oxidation states could also be carried out by coupling with ion  
 209 exchange chromatography<sup>67</sup> although these couplings remain *ex situ* to date. For single particle  
 210 analysis, several technical aspects must be optimized, such as the injection system (nebulizer and  
 211 spray chamber types). In addition, the atomization process of single particles and the effect of particle  
 212 composition on signal intensity are still not well understood and thus require further research. Finally,  
 213 a better understanding of the hydrodynamics of the electrochemical flow cell used in the AESEC  
 214 technique can be obtained by numerical modeling.<sup>68</sup>

215

216 **Conflict of interest statement**

217 Nothing declared.

218

219 **Acknowledgment**

220 This work was supported by Agence Nationale de Recherche - Jeune Chercheur et Jeune Chercheuse  
221 (ANR-JCJC) #ANR-22CE08-0015-01 (QUEENE). The authors acknowledge financial support from  
222 Sorbonne Université and the Centre *National de la Recherche Scientifique* (CNRS), France.

223

224 **References**

225 Papers of particular interest, published within the period of review, have been highlighted as:

226 \* of special interest \*\* of outstanding interest

---

<sup>1</sup> Ogle K, Weber S, “Anodic dissolution of 304 stainless steel using atomic emission spectroelectrochemistry “, *J. Electrochem. Soc.*, 2000, **147**(5):1770-1780; <https://doi.org/10.1149/1.1393433>

\*\*

<sup>2</sup> Kasian O, Geiger S, Mayrhofer KJJ, Cherevko S, “Electrochemical on-line ICP-MS in electrocatalysis research”, *Chem. Rec.*, 2019, **19**:2130:2142; <https://doi.org/10.1002/tcr.201800162>

This article reviews the recent advances in on-line ICP-MS focusing on the degradation mechanism of electrocatalysis. Insights on future applications of the on-line ICP-MS technique to investigate materials in the energy field are provided.

\*\*

<sup>3</sup> Ogle K, “Atomic emission spectroelectrochemistry: Real-time rate measurements of dissolution, corrosion, and passivation”, *Corrosion*, 2019, **75**(12):1398-1419; <https://doi.org/10.5006/3336>

This article reviews the principles and applications of the AESEC technique primarily for corrosion investigation. It introduces a brief history and technical evolution of the AESEC technique from the developer’s point of view. Detailed explanations are provided on methodological approaches to determine element-resolved electrochemical process.

<sup>4</sup> Choudhary S, Ogle K, Gharbi O, Thomas S, Birbilis N, “Recent insights in corrosion science from atomic spectroelectrochemistry”, *Electrochem. Sci., Adv.*, 2021, **e2100196**; <https://doi.org/10.1002/elsa.202100196>

<sup>5</sup> Gharbi O, Hirsh O, Chapon P, Stankova A, “Inductively coupled plasma optical emission spectroscopy”, *Materials Characterization*, ASM handbook, 2019

<sup>6</sup> Olge K, Lodi P, Storhaye A, “Méthode d’analyse d’un échantillon métallique par dissolution de sa surface, et dispositif pour sa mise en œuvre”, Patent, 1992, FR2689244A1.

<sup>7</sup> Laurent B, Gruet N, Gwinner B, Miserque F, Tabarant M, Ogle K, “A direct measurement of the activation potential of stainless steels in nitric acid”, *J. Electrochem. Soc.*, 2017, **164**(9):C481-C487; <https://doi.org/10.1149/2.0081709jes>

- <sup>8</sup> Li X, Zhou P, Ogle K, Proch S, Paliwal M, Jansson An, Westlinder J, “Transient stainless-steel dissolution and its consequences on ex-situ bipolar plate testing procedures”, *Int. J. Hyd. Ener.*, 2022, **45**(1):984-995; <https://doi.org/10.1016/j.ijhydene.2019.10.191>
- <sup>9</sup> Li X, Ogle K, “The passivation of Ni-Cr-Mo alloys: Time resolved enrichment and dissolution of Cr and Mo during passive-active cycles”, *J. Electrochem. Soc.*, 2019, **166**(11):C3179-C3185; <https://doi.org/10.1149/2.0201911jes>
- <sup>10</sup> Lutton K, Gusieva K, Ott N, Birbilis N, Scully JR, “Understanding multi-element alloy passivation in acidic solutions using operando methods”, *Electrochem. Commu.*, 2017, **80**:44-47; <https://doi.org/10.1016/j.elecom.2017.05.015>
- <sup>11</sup> Serdechnova M, Volovitch P, Brisset Fr, Ogle K, “On the cathodic dissolution of Al and Al alloys”, *Electrochim. Acta*, 2014, **124**:9-16; <https://doi.org/10.1016/j.electacta.2013.09.145>
- <sup>12</sup> Han J, Ogle K, “Cathodic dealloying of  $\alpha$ -phase Al-Zn in slightly alkaline chloride electrolyte and its consequence for corrosion resistance”, *J. Electrochem. Soc.*, 2018, **165**(7):C334-C342; <https://doi.org/10.1149/2.0581807jes>
- <sup>13</sup> Rossrucker L, Mayrhofer KJJ, Frankel G, Birbilis N, “Investigating the real time dissolution of Mg using online analysis by ICP-MS”, *J. Electrochem. Soc.*, 2014, **161**(3):C115-C119; <https://doi.org/10.1149/2.064403jes>
- <sup>14</sup> Lebouil S, Gharbi O, Volovitch P, Ogle K, “Mg dissolution in phosphate and chloride electrolytes: Insight into the mechanism of the negative difference effect”, *Corrosion*, 2015, **71**(2):234-241; <https://doi.org/10.5006/1459>
- <sup>15</sup> Vu TN, Mokaddem M, Volovitch P, Ogle K, “The anodic dissolution of zinc and zinc alloys in alkaline solution. II. Al and Zn partial dissolution from 5% Al-Zn coatings”, *Electrochim. Acta*, 2012, **74**:130-138; <https://doi.org/10.1016/j.electacta.2012.04.037>
- <sup>16</sup> Han J, Ogle K, “Dealloying of MgZn<sub>2</sub> intermetallic in slightly alkaline chloride electrolyte and its significance in corrosion resistance”, *J. Electrochem. Soc.*, **164**(14):C952-C961; <https://doi.org/10.1149/2.0341714jes>
- <sup>17</sup> Zou P, Ogle K, “The corrosion of copper and copper alloys”, in *Encyclopedia of Interfacial Chemistry – Surface Science and Electrochemistry*, 2018, **6**:478-489
- <sup>18</sup> Zhou P, Hutchison MJ, Erning JW, Scully J, Ogle K, “An in situ kinetic study of brass dezincification and corrosion”, *Electrochim. Acta*, 2017, **229**:141-154; <https://doi.org/10.1016/j.electacta.2017.01.078>
- <sup>19</sup> Choudhary S, Thomas S, Macdonald DD, Birbilis N, “Growth kinetics of multi-oxide passive film formed upon the multi-principal element alloy AlTiVCr: Effect of transpassive dissolution of V and Cr”, *J. Electrochem. Soc.*, 2021, **168**:051506; <https://doi.org/10.1149/1945-7111/ac0018>
- <sup>20</sup> Choudhary S, Birbilis N, Thomas S, “Evolution of passivity for the multi-principal element alloy CoCrFeNi with potential, pH, and exposure in chloride solution”, *Corrosion*, 2022, **78**(1):49-57; <https://doi.org/10.5006/3902>
- <sup>21</sup> Choudhary S, O’Biren S, Thomas S, Gupta RK, Birbilis N, “On the dynamic passivity and corrosion resistance of a low cost and low density multi-principal-element alloy produced via commodity metals”, *Electrochim. Commu.*, 2021, 125:106989; <https://doi.org/10.1016/j.elecom.2021.106989>
- <sup>22</sup> Luo H, Li Z, Mingers AM, Raabe D, “Corrosion behavior of an equiatomic CoCrFeMnNi high-entropy alloy compared with 304 stainless steel in sulfuric acid solution”, *Corros. Sci.*, 2018, 134:131-139; <https://doi.org/10.1016/j.corsci.2018.02.031>
- <sup>23</sup> Li X, Zhou P, Feng H, Jiang Z, Li H, Ogle K, “Spontaneous passivation of the CoCrFeMnNi high entropy alloy in sulfuric acid solution: The effects of alloyed nitrogen and dissolved oxygen”, *Corros. Sci.*, 2022, **196**:110016; <https://doi.org/10.1016/j.corsci.2021.110016>
- <sup>24</sup> Li X, Han J, Lu P, Saal JE, Olson GB, Frankel GS, Scully JR, Ogle K, “Communication-Dissolution and passivation of a Ni-Cr-Fe-Ru-Mo-W high entropy alloy by elementally resolved electrochemistry”, *J. Electrochem. Soc.*, 2020, **167**:061505; <https://doi.org/10.1149/1945-7111/ab7f86>
- <sup>25</sup> Gharbi O, Jiang D, Feenstra DR, Dairy SK, Wu Y, Hutchinson CR, Birbilis N, “On the corrosion of additively manufactured aluminium alloy AA2024 prepared by selective laser melting”, *Corros. Sci.*, 2018, **143**:93-106; <https://doi.org/10.1016/j.corsci.2018.08.019>
- <sup>26</sup> Klemm SO, Karschin A, Schuppert AK, Topalov AA, Mingers AM, Katsounaros I, and Mayrhofer KJJ, “Time and potential resolved dissolution analysis of rhodium using a microelectrochemical flow cell coupled to an ICP-MS”, *J. Electroanal. Chem.*, 2012, **677-680**: 50-55; <https://doi.org/10.1016/j.jelechem.2012.05.006>
- <sup>27</sup> Cherevko S, Zeradjanin AR, Topalov AA, Kulyk N, Katsounaros I, Mayrhofer KJJ, “Dissolution of noble metals during oxygen evolution in acidic media”, *Chem. Cat. Chem.*, 2014, **6**:2219-2223; <https://doi.org/10.1002/cctc.201402194>
- <sup>28</sup> Hodnik N, Balizzzone C, Polymeros G, Geiger S, Grote JP, Cherevko S, Mingers A, Zeradjanin A, Mayrhofer KJJ, “Platinum recycling going green via induced surface potential alteration enabling fast and efficient dissolution”, *Nature Commu.*, 2016, **7**:13164; <https://doi.org/10.1038/ncomms13164>

---

<sup>29</sup> Gharbi O, Birbilis N, Ogle K, “In-situ monitoring of alloy dissolution and residual film formation during the pretreatment of Al-alloy AA2024-T3”, *J. Electrochem. Soc.*, 2016, **163**:C240-C251; <https://doi.org/10.1149/2.1121605jes>

<sup>30</sup> Gharbi O, Birbilis N, Ogle K, “Li reactivity during the surface pretreatment of Al-Ai alloy AA2025-T3”, *Electrochim Acta*, 2017, **243**:207-219; <https://doi.org/10.1016/j.electacta.2017.05.038>

<sup>31</sup> Bin Mohamad Sultan B, Thierry D, Torrescano-Alvarez JM, Ogle K, “Selective dissolution during acid pickling of aluminum alloys by element-resolved electrochemistry”, *Electrochim. Acta*, 2022, **404**:139737; <https://doi.org/10.1016/j.electacta.2021.139737>

\*

<sup>32</sup> Bin Mohamad Sultan B, Thierry D, Ogle K, “On the dissolution rates and mechanisms of Al-Mg and Al-Cu alloys during acid pickling using element-resolved electrochemistry”, *Electrochim. Acta*, 2023, **444**:141961; <https://doi.org/10.1016/j.electacta.2023.141961>

This article shows the advantages of the AESEC technique in the field of surface pretreatment prior to the conversion coating process. The real-time selective dissolution mechanism with the information of enriched/depleted elements was investigated for Al-Cu and Al-Mg alloys in acid pickling experiments. It also showed the possibilities of qualitative monitoring of the particles using the AESEC technique.

<sup>33</sup> Klemm SO, Pust SE, Hassel AW, Hüpkes J, Mayrhofer KJJ, “Electrochemical texturing of Al-doped ZnO thin films for photovoltaic applications”, *J. Solid State Electrochem.*, 2012, **16**:283-290; <https://doi.org/10.1007/s10008-011-1313-z>

<sup>34</sup> Lebouil S, Duboin A, Monti F, Tabeling P, Volovitch P, Ogle K, “A novel approach to on-line measurement of gas evolution kinetics: Application to the negative difference effect of Mg in chloride solution”, *Electrochim. Acta*, 2014, **124**:176-182; <https://doi.org/10.1016/j.electacta.2013.07.131>

<sup>35</sup> Han J and Ogle K, “Hydrogen evolution and elemental dissolution by combined gravimetric method and atomic emission spectroelectrochemistry”, *J. Electrochem. Soc.*, 2019, **166**(11):C3068-C3070; <https://doi.org/10.1149/2.0091911jes>

<sup>36</sup> Dou B, Li X, Han J, Ogle K, “Operando kinetics of hydrogen evolution and elemental dissolution I: The dissolution of galvanized steel in hydrochloric acid”, *Corros. Sci.*, 2023, **214**:111007; <https://doi.org/10.1016/j.corsci.2023.111007>

\*\*

<sup>37</sup> Dou B, Li X, Han J, Ogle K, “Operando kinetics of hydrogen evolution and elemental dissolution II: A time resolved mass-charge balance during the anodic dissolution of magnesium with variable iron content”, *Corros. Sci.*, 2023, **217**:111095; <https://doi.org/10.1016/j.corsci.2023.111095>

This article describes a novel approach for the simultaneous measurement of hydrogen evolution reaction (HER) and elemental dissolution rates in the case of anodic hydrogen production (*i.e.*, negative difference effect) of nominally pure Mg. The results demonstrate the analytical capabilities of the AESEC-gravimetric technique through experiments that verify and validate this hyphenated analytical technique.

\*

<sup>38</sup> Molina DE, Wall N, Beyenal H, Ivory CF, “Flow injection electrochemical quartz crystal microbalance with ICP-OES detection: Recovery of silver by electrodeposition with redox replacement in a flow cell”, *J. Electrochem. Soc.*, 2021, **168**:056518; <https://doi.org/10.1149/1945-7111/abfcdd>

This article discusses a novel on-line FI-EQCM-ICP-OES that enables electrochemical deposition and stripping with mass detection and elemental analysis. The authors used this technique for the investigation of mass changes on the electrode during electrodeposition and open circuit times in each EDRR cycle in flowing solutions.

<sup>39</sup> Ogle K, Tomandl A, Meddahi N, “In situ monitoring of dissolution-precipitation mechanisms using coupled quartz crystal microbalance/atomic emission spectroelectrochemistry, in EFC 54, Innovative Pre-treatment Techniques to Prevent Corrosion of Metallic Surfaces; Woodhead Publishing Ltd: Cambridge, 2007; p 158.

<sup>40</sup> Hamm D, Ogle K, Olsson COA, Weber W, Landolt D, “Passivation of Fe-Cr alloys studied with ICP-AES and EQCM”, *Corros. Sci.*, 2002, **44**:1443-1456; [https://doi.org/10.1016/S0010-938X\(01\)00147-0](https://doi.org/10.1016/S0010-938X(01)00147-0)

<sup>41</sup> Gabrielli C, Keddam M, Minouflet-Laurent F, Ogle K, Perrot H, “Investigation of zinc chromation. I. Application of QCM-ICP coupling”, *Electrochim. Acta*, 2003, **48**:965 (2003); [https://doi.org/10.1016/S0013-4686\(02\)00809-5](https://doi.org/10.1016/S0013-4686(02)00809-5)

- <sup>42</sup> Gharbi O, Ogle K, Han J, “On the chemistry of the conversion coatings”, *Encyclopedia of Solid-Liquid Interfaces, Reference Module in Chemistry, Molecular Sciences and Chemical Engineering* (2023); <https://doi.org/10.1016/B978-0-323-85669-0.00091-X>
- <sup>43</sup> Ogle K, Tomandl A, Meddahi N, Wolpers M, “The alkaline stability of phosphate coatings I: ICP atomic emission spectroelectrochemistry”, *Corros. Sci.*, 2004, **46**:979-995; [https://doi.org/10.1016/S0010-938X\(03\)00182-3](https://doi.org/10.1016/S0010-938X(03)00182-3)
- <sup>44</sup> Ogle K, Tomandl A, Meddahi N, Wolpers M, “The alkaline stability of phosphate coatings II: in situ Raman spectroscopy”, *Corros. Sci.*, 2004, **46**:997-1011; [https://doi.org/10.1016/S0010-938X\(03\)00183-5](https://doi.org/10.1016/S0010-938X(03)00183-5)
- <sup>45</sup> Vivier V, Orazem ME, “Impedance analysis of electrochemical systems”, *Chem. Rev.*, 2022, **122**:11131-11168; <https://doi.org/10.1021/acs.chemrev.1c00876>
- <sup>46</sup> Shkirskiy V, Ogle K, “A novel coupling of electrochemical impedance spectroscopy with atomic emission spectroelectrochemistry: Application to the open circuit dissolution of zinc”, *Electrochim. Acta*, 2015, **168**:167-172; <https://doi.org/10.1016/j.electacta.2015.03.171>
- <sup>47</sup> Han J, Gerard AY, Lu P, Saal JE, Ogle K, Scully JR, “Elementally resolved dissolution kinetics of a Ni-Fe-Cr-Mn-Co multi-principal element alloy in sulfuric acid using AESEC-EIS”, *J. Electrochem. Soc.*, 2022, **167**:081507; <https://doi.org/10.1149/1945-7111/ac862b>
- <sup>48</sup> Han J, Ogle K, “The anodic and cathodic dissolution of  $\alpha$ -phase Zn-68Al in alkaline media”, *Corros. Sci.*, 2019, **148**:1-11; <https://doi.org/j.corsci.2018.11.033>
- \*\*
- <sup>49</sup> Han J, Vivier V, Ogle K, “Refining anodic and cathodic dissolution mechanisms: combined AESEC-EIS applied to Al-Zn pure phase in alkaline solution”, *npj Mater. Degrad.*, 2020, **4**:19; <https://doi.org/10.1038/s41529-020-0123-0>  
**This article highlighted the use of AESEC-EIS to probe further the element-specific dissolution mechanisms. It is demonstrate that the anodic and cathodic reaction mechanisms can be distinguished by the AESEC-EIS methodology. The nature of the charge-transfer mechanism depending on the applied potential could be identified by this technique.**
- <sup>50</sup> Han J, Ogle K, “Elementally resolved electrochemical impedance spectroscopy: dissolution kinetics of Ni, Cr-containing high-entropy alloys”, *Eurocorr* 2022.
- <sup>51</sup> Bockris JO'M, Drazic D, Despic AR, “The electrode kinetics of the deposition and dissolution of iron”, *Electrochim. Acta*, 1961, **4**:325-361; [https://doi.org/10.1016/0013-4686\(61\)80026-1](https://doi.org/10.1016/0013-4686(61)80026-1)
- <sup>52</sup> Gabrielli C, Tribollet B, “A transfer function approach for a generalized electrochemical impedance spectroscopy”, *J. Electrochem. Soc.*, 1994, **141**:1147; <https://doi.org/10.1149/1.2054888>
- <sup>53</sup> Knöppel J, Zhang S, Speck FD, Mayrhofer KJJ, Scheu C, Cherevko S, “Time-resolved analysis of dissolution phenomena in photoelectrochemistry – a case study of WO<sub>3</sub> photocorrosion”, *Electrochem. Commu.*, 2018, **96**:53-56; <https://doi.org/10.1016/j.elecom.2018.09.008>
- <sup>54</sup> Dworschak D, Brunnhofer C, Valtiner M, “Photocorrosion of ZnO single crystals during electrochemical water splitting”, *ACS Appl. Mater. Interfaces*, 2020, **12**:51530-51536; <https://doi.org/10.1021/acsami.0c15508>
- <sup>55</sup> Zhang S, Rohloff M, Kasian O, Mingers AM, Mayrhofer KJJ, Fischer A, Scheu C, Cherevko S, “Dissolution of BiVO<sub>4</sub> photoanodes revealed by time-resolved measurements under photoelectrochemical conditions”, *J. Phys. Chem. C*, 2019, **123**:23410-23418; <https://doi.org/10.1021/acs.jpcc.9b07220>
- <sup>56</sup> Kasian O, Geiger S, Li T, Grote JP, Schweinar K, Zhang S, Scheu C, Raabe D, Cherevko S, Gault B, Mayrhofer KJJ, “Degradation of iridium oxides via oxygen evolution from the lattice: correlating atomic scale structure with reaction mechanisms”, *Energy Environ. Sci.*, 2019, **12**:3548; <https://doi.org/10.1039/c9ee01872g>
- <sup>57</sup> Spanos I, Auer AA, Neugebauer S, Deng X, Tüysüz H, Schlögl R, “Standardized benchmarking of water splitting catalysts in a combined electrochemical flow cell/inductively coupled plasma-optical emission spectrometry (ICP-OES) setup”, *ACS Catal.*, 2017, **7**:3768-3778; <https://doi.org/10.1021/acscatal.7b00632>
- <sup>58</sup> Mayrhofer KJJ, Hartl K, Juhart V, Arenz M, “Degradation of carbon-supported Pt bimetallic nanoparticles by surface segregation”, *J. Am. Chem. Soc.*, 2009, **131**:16348-16349; <https://doi.org/10.1021/ja9074216>
- <sup>59</sup> Li T, Kasian O, Cherevko S, Zhang S, Geiger S, Scheu C, Felfer P, Raabe D, Gault B, Mayrhofer KJJ, “Atomic-scale insights into surface species of electrocatalysts in three dimensions”, *Nature Catalysis*, 2018 **1**:300-305; <https://doi.org/10.1038/s41929-018-0043-3>
- <sup>60</sup> Lopes PP, Zorko M, Hawthorne KL, Connel JG, Ingram BJ, Strmcnik D, Stamenkovic VR, Markovic NM, “Real-time monitoring of cation dissolution/deintercalation kinetics from transition-metal oxides in organic environments”, *J. Phys. Chem. Lett.*, 2018, **6**:9(17):4935-4940; <https://doi.org/10.1021/acs.jpclett.8b01936>
- <sup>61</sup> Buchheit RG, Grant RP, Hlava PF, Mckenzie B, Zender GL, “Local dissolution phenomena associated with S phase (Al<sub>2</sub>CuMg) particles in aluminum alloy 2024-T3”, *J. Electrochem. Soc.*, 1997, **144**(8):2621; <https://doi.org/10.1149/1.1837874>

- 
- <sup>62</sup> Mokaddem M, Volovitch P, Rechou F, Oltra R, Ogle K, “The anodic and cathodic dissolution of Al and Al-Cu-Mg alloy”, *Electrochim. Acta*, 2010, **55**:3779-3786; <https://doi.org/10.1016/j.electacta.2010.01.079>
- <sup>63</sup> Serdechnova M, Volovitch P, Ogle K, “Atomic emission spectroelectrochemistry study of the degradation mechanism of model high-temperature paint containing sacrificial aluminum particles”, *Surf. & Coat. Tech.*, 2012, **206**(8-9): 2133-2139; <https://doi.org/10.1016/j.surfcoat.2011.09.044>
- <sup>64</sup> Gharbi O, “In situ investigation of elemental corrosion reactions during the surface treatment of Al-Cu and Al-Cu-Li alloys”, Université Pierre et Marie Curie – Paris VI, 2016; tel-01535612
- <sup>65</sup> Han J, Gharbi O, “Current state of electrochemical techniques and corrosion rate analysis for next-generation materials”, *Current Opinion in Electrochemistry*, 2022, **36**:101131; <https://doi.org/10.1016/j.coelec.2022.101131>
- <sup>66</sup> Dworschak D, Brunnhofer C, Valtiner M, “Complementary electrochemical ICP-MS flow cell and in-situ AFM study of the anodic desorption of molecular adhesion promoters”, *Appl. Surf. Sci.*, 2021, **570**:151015; <https://doi.org/10.1016/j.apsusc.2021.151015>
- <sup>67</sup> Xing L, Jerkiewicz G, Beauchemin D, “Ion exchange chromatography coupled to inductively coupled plasma mass spectrometry for the study of Pt electro-dissolution”, *Anal. Chimica Acta*, 2013, **785**:16-21; <https://doi.org/10.1016/j.aca.2013.04.048>
- <sup>68</sup> Shkirskiy V, Maciel P, Deconinck J, Ogle K, “On the time resolution of the atomic emission spectroelectrochemistry method”, *J. Electrochem. Soc.*, 2016, **163**(3):C37-C44; <https://doi.org/10.1149/2.0991602jes>